Sub-slab seismic anisotropy and mantle flow beneath the Caribbean and Scotia subduction zones: Effects of slab morphology and kinematics

Colton Lynner *, Maureen D. Long

Department of Geology and Geophysics, Yale University, PO Box 208109, New Haven, CT 06520, USA

A B S T R A C T

Subduction systems are vitally important to plate tectonics and mantle convection, but questions remain about many aspects of subduction dynamics, particularly the nature of sub-slab mantle flow. Observations of seismic anisotropy can shed light on the pattern of mantle flow in subduction systems, but major uncertainties remain regarding the interpretation of sub-slab anisotropy. Here, we present measurements of shear wave splitting due to anisotropy in the sub-slab mantle beneath the Caribbean and Scotia subduction zones. These subduction systems are morphologically similar, with high arc curvature and short arc length, but there are differences between them in terms of their kinematic and tectonic settings. We apply the source-side shear wave splitting technique to direct teleseismic S phases originating from slab earthquakes. We restrict our analysis to seismic stations at which we have examined the receiver-side splitting in detail to ensure accurate corrections for anisotropy in the upper mantle beneath the station. We observe a well-defined pattern of trench-parallel fast directions (ϕ) in the northern half of the Caribbean subduction zone, with a transition to dominantly trench-perpendicular ϕ at the southern end. There is more scatter in the measurements for Scotia, but we observe generally trench-parallel ϕ in the northern portion of the subduction system, with a mix of trench-parallel, -perpendicular, and -oblique fast directions to the south. Our preferred interpretation of these splitting patterns is that they reflect 3-D return flow of the sub-slab mantle due to trench rollback. In both systems, we infer that sub-slab flow is being driven from south to north. Beneath Scotia, this is likely driven by differential migration of the Scotia trench along strike. Beneath the Caribbean, we hypothesize that mantle flow around the southern edge of the slab is inhibited by the presence of the South American continental keel, enabling trench-perpendicular stretching in the sub-slab mantle and forcing mantle flow to escape to the north. The similarities and differences we observe between the two systems yield insight into the relative contributions of slab morphology and plate kinematics in controlling mantle flow beneath subducting slabs.

© 2012 Elsevier B.V. All rights reserved.

1. Introduction

Subduction zones are among the most geodynamically and tectonically complicated regions on the planet. A tremendous amount of research has been aimed at constraining the structure and dynamics of subduction zones (overviews of recent work can be found in Zhao, 2001; van Keken, 2003; King, 2007; Billen, 2008). Despite this effort to fully understand the subduction process, many aspects of subduction systems remain poorly understood. One such aspect is the pattern of mantle flow beneath subducting slabs. Understanding the controls on the flow of sub-slab mantle may yield crucial insights into the geodynamics of subduction.

Measurements of seismic anisotropy represent the most direct observational constraints we can place on patterns of mantle flow (e.g., Silver, 1996; Savage, 1999; Long and Becker, 2010). When olivine, the dominant upper mantle mineral, is deformed under upper mantle conditions, individual crystal grains tend to develop a statistical preferred orientation (e.g., Karato et al., 2008, and references therein). Under most conditions of deformation relevant to the upper mantle, the fast axes of olivine tend to align with the direction of maximum strain (e.g., Karato et al., 2008). When a shear wave propagates through an anisotropic region of the upper mantle, it undergoes shear wave splitting (e.g., Vinnik et al., 1989; Silver and Chan, 1991) and the quasi-shear wave polarizations and the delay time between them can constrain the geometry of mantle deformation.

Studies of shear wave splitting due to anisotropy in the sub-slab mantle in most subduction zones often find evidence for trench-parallel fast splitting directions. This type of splitting

* Corresponding author.
E-mail address: colton.lynner@yale.edu (C. Lynner).

pattern has been documented in many individual subduction zones (e.g. Russo and Silver, 1994; Peyton et al., 2001; Civello and Margheriti, 2004; Foley and Long, 2011; Di Leo et al., 2012) and also dominates the sub-slab splitting signal in subduction systems globally (Long and Silver, 2008, 2009a). This observation, however, contradicts the predictions of the simplest 2-D entrained flow models, which would predict trench-perpendicular fast directions for simple olivine LPO scenarios (e.g., Russo and Silver, 1994; Long and Silver, 2009a; Long and Becker, 2010). Several different models have been proposed to explain this discrepancy, including trench-parallel flow beneath slabs (Russo and Silver, 1994; Long and Silver, 2008; Paczkowski, 2012), aligned serpentinized cracks within slabs (Faccenda et al., 2008; Healy et al., 2009), B-type olivine fabric in the sub-slab mantle (Jung et al., 2009), or a layer of entrained asthenosphere with strong radial anisotropy beneath slabs (Song and Kawakatsu, 2012). To first order, all of these models are generally consistent with the global observation of dominantly trench-parallel sub-slab fast directions. In order to discriminate among these models, detailed shear wave splitting datasets with good spatial and depth coverage that utilize raypaths with a range of back-azimuths and incidence angles are needed.

The most common methodology for examining shear wave splitting in the sub-slab mantle involves measuring the splitting of SK(K)S phases arriving at seismic stations located above the subduction zone and applying a correction for the effect of anisotropy in the mantle wedge (e.g., Long and Silver, 2009a). This approach is problematic, however, when trying to place detailed constraints on sub-slab anisotropy. Data sets are limited by the location of seismic instrumentation, which leads to poor spatial sampling of the sub-slab mantle. Another problem lies in the fact that SK(K)S phases reflect the integrated effect of anisotropy in the sub-slab mantle, the subducting slab, the mantle wedge, and the overriding plate. While corrections for wedge anisotropy based on local S splitting studies can be applied, these corrections are inexact, as the wedge splitting signal is usually very complex (Long and Silver, 2008). Even if the effect of wedge anisotropy can be correctly accounted for, this approach cannot place constraints on the depth distribution of

anisotropy in the sub-slab mantle. An alternative method for measuring sub-slab anisotropy utilizes the so-called source-side shear wave splitting technique (e.g., Russo and Silver, 1994), which measures splitting for teleseismic S phases originating from earthquakes in the subducting slab. As long as the effect of upper mantle anisotropy beneath the receiver is correctly accounted for, this method can provide direct constraints on anisotropy beneath subducting slabs, and can provide information about the variation of anisotropy with depth and along strike.

Here we present detailed source-side shear wave splitting measurements for earthquakes originating in the subducting slabs beneath the Caribbean and Scotia subduction zones. These two subduction systems exhibit similar morphologies, with short arc length and high arc curvature, but are different in terms of their plate kinematics and boundary conditions. A key question is whether the highly curved morphologies of these trench/slab systems are associated with efficient flow around the slab edge(s), and if so, whether the slab curvature is a cause or a result of such a flow pattern. A comparison of sub-slab splitting between these subduction systems also offers an opportunity to investigate whether sub-slab anisotropy and mantle flow is mainly controlled by slab morphology, plate kinematics, or a combination of these factors. The source-side splitting measurements presented here provide a detailed look at the along-strike and depth variation in measured splitting parameters, and the good raypath coverage of our datasets allows us to test the predictions of the various models for sub-slab anisotropy in the context of the Scotia and Caribbean subduction systems.

2. Tectonic setting

The Caribbean and Scotia subduction zones are characterized by short arc length (~850 km), high trench curvature, and very similar slab morphologies, with slab dips ranging from ~32° to ~56° (e.g., Schellart, 2007). They also represent the only locations where the South American plate is currently being subducted (Fig. 1).
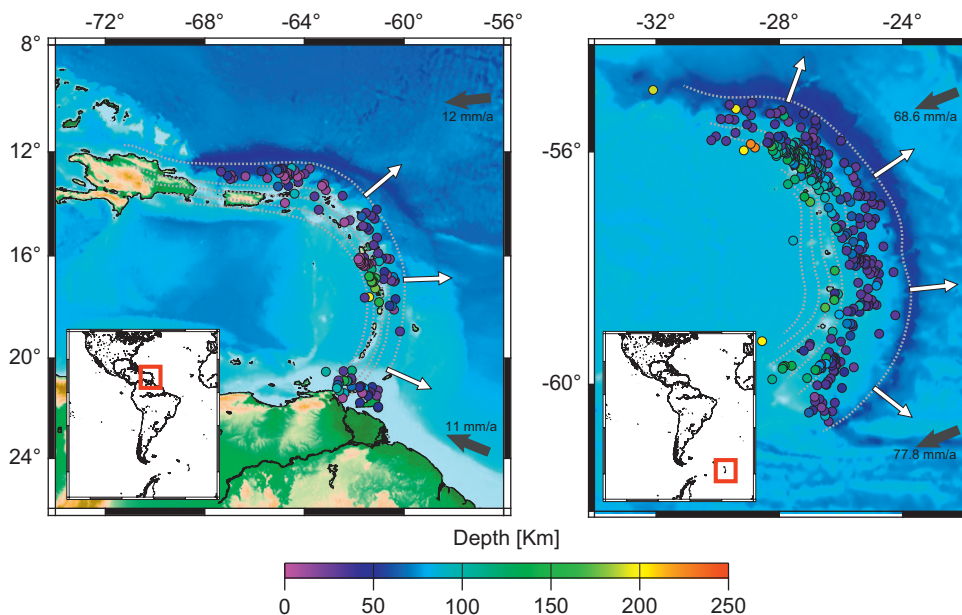
Fig. 1. Tectonic setting of the Caribbean (left) and Scotia (right) subduction zones. Circles denote slab seismicity, with event depth denoted by color. We show events of magnitude greater than Mw=5.0 for a 10 yr time span from 2000 to 2010 for event depths greater than 25 km. The gap in seismicity in the Caribbean is clearly visible from ~11°N–14°N as is the drastic difference in the amount of seismicity between the two subduction zones. Dashed lines show contours of slab seismicity, in intervals of 50 km, from Gudmundsson and Sambridge (1998). Black arrows show the direction of motion of the downgoing plate relative to the overlying plate, while white arrows are a schematic representation of the migration of the trenches relative to the South American plate. (For interpretation of the references to color in this figure legend, the reader is referred to the web version of this article.)

In a reference frame in which the South American plate is fixed, both subduction zones are experiencing trench retreat, with both trenches migrating to the east. While the two subduction zones are similar in respect to their morphologies, they do differ with regard to their tectonic settings and plate kinematics. The Caribbean subduction zone is bounded to the south by the continental part of the South American plate and to the north by oceanic lithosphere, while the Scotia arc is located in a completely oceanic environment. At the Caribbean trench, the downgoing plate is subducting at a rate of ~11 mm/yr beneath the overriding Caribbean plate (DeMets et al., 1990). The age of the downgoing lithosphere ranges from 120 Ma at the southern end of the subduction system to 100 Ma at the northern end (Heuret and Lallemand, 2005). The trench is migrating to the east at a rate of approximately ~11 mm/yr (with respect to the South American plate) but is actually advancing at a rate of 27 mm/yr in a Pacific hotspot reference frame (Heuret and Lallemand, 2005). At the northern end of the Caribbean subduction zone, the high trench curvature results in an oblique collision associated with strike-slip motion in the northeasternmost portion of the Caribbean–North American plate boundary (e.g., Mann et al., 2002). The strike-slip deformation of the overriding plate is unlikely to have a large impact on sub-slab mantle flow, however.

In contrast, the Scotia subduction zone does not have significant transform motion at its northern end. At the Scotia trench the downgoing plate is subducting at a rate of ~74 mm/yr (Thomas et al., 2003), and the age of the subducting lithosphere ranges from 33 Ma to 40 Ma (Heuret and Lallemand, 2005). The rate of trench migration for Scotia ranges from −17 mm/yr (local trench advance) to 49 mm/yr in a Pacific hotspot reference frame (Heuret and Lallemand, 2005). Again in contrast to the Caribbean subduction system, there is a well-developed backarc spreading center in the overriding plate, with a full spreading rate of ~65 mm/yr (Thomas et al., 2003). A key goal of this study is to examine whether the characteristics that are different between the subduction zones (e.g. tectonic setting at slab edges, plate kinematic variables) play a role in controlling the anisotropy beneath the subducting slabs.

The source-side splitting technique used in this study relies on teleseismic phases originating from earthquakes within the subducting slabs and does not require seismic stations deployed in the Caribbean and Scotia regions to observe sub-slab anisotropy. The spatial distribution of relatively large earthquakes (Mw > 5) in the slabs thus dictates the data coverage we can obtain. The Scotia subduction zone exhibits a large amount of slab seismicity (Fig. 1) along most of its width, although there is less seismicity in the southernmost part of the subduction zone. The Caribbean slab is less seismogenic in general and exhibits a prominent gap in seismicity in the middle part of the subduction zone (Fig. 1). While the Caribbean slab is less seismically active than its Scotia counterpart, there is nonetheless enough seismicity to characterize the seismic anisotropy beneath most of the subducting slab (Fig. 1).

3. Methods and data

3.1. The source-side splitting technique

Source-side splitting refers to the technique in which teleseismic S waves are used to examine anisotropy in the region where the waves originated. The technique was first implemented by Russo and Silver (1994), and has since been applied to examine anisotropy in subduction zones (Müller et al. (2008); Russo, 2009; Russo et al., 2010; Foley and Long, 2011; Di Leo et al., 2012) as well as other settings such as spreading ridges (Nowacki et al., 2012). Teleseismic S waves (at epicentral distances 40°–80°)

potentially sample anisotropy in the upper mantle beneath the source as well as beneath the receiver; we assume that the lower mantle is isotropic (e.g. Meade et al., 1995). In order to isolate the anisotropy near the source, the receiver-side anisotropic signal must be well constrained and removed from the incoming S wave. A crucial aspect of the technique is that the receiver-side splitting must be well characterized and simple, as inaccurate corrections for receiver-side anisotropy can bias estimates of source-side splitting.

In order to identify good candidate stations for our study, we examined SK(K)S splitting at 108 broadband seismic stations located at epicentral distances of 40°–80° from the Caribbean and Scotia source regions (Fig. 2). In order to characterize the receiver-side splitting signal, we examined SK(K)S phases for events of magnitude Mw ≥ 5.8 at epicentral distances between 90° and 130°. Through this investigation of SK(K)S splitting parameters at candidate stations, we identified two types of simple SK(K)S patterns that correspond to simple anisotropic geometries and allow for accurate receiver-side corrections. The first and simplest is a pattern of null SK(K)S arrivals – that is, phases that are not split – from many different backazimuths with no (or very few) split arrivals (e.g., Lynner and Long, 2012). This indicates that an apparently isotropic structure beneath the station, in which the upper mantle is isotropic, is characterized by destructive interference from different anisotropic layers, or exhibits a vertical axis of anisotropic symmetry that leaves the incoming waves unsplit. This pattern of upper mantle anisotropy requires no receiver-side correction.

The second pattern of simple upper mantle anisotropy which allows for accurate receiver-side correction is a splitting pattern in which similar splitting parameters are recorded at a number of different backazimuths, indicating a single horizontal layer of anisotropy. SK(K)S splitting patterns that vary in delay time or fast axis with backazimuth indicate a dipping axis of symmetry or multiple layers of anisotropy (e.g., Silver and Savage, 1994) and it is difficult to carry out accurate receiver-side corrections for stations with such complex splitting patterns. For this reason, we have chosen to exclude stations with complex SK(K)S splitting from this study. Of the 108 stations at which we carried out
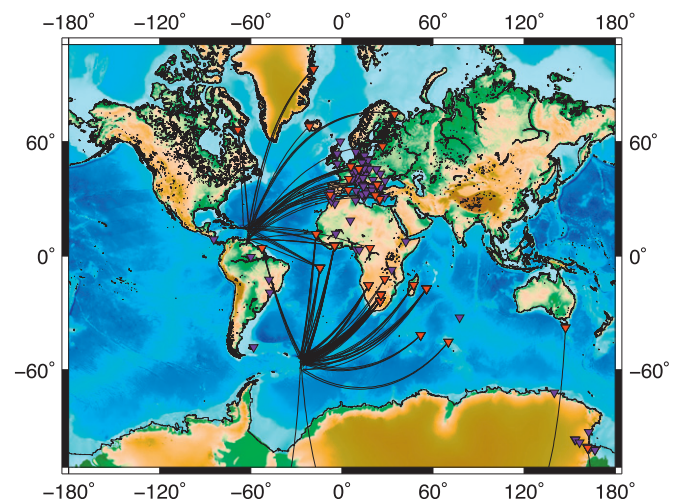
Fig. 2. Map of the stations examined using SK(K)S phases in this study. Red triangles denote stations that had adequate backazimuthal coverage and showed either a simple or a null pattern of splitting and were thus used to make source-side measurements. Purple triangles represent stations that had either insufficient backazimuthal coverage or showed a complicated pattern of splitting and could thus not be used to examine the source regions. Thin black lines indicate source-to-receiver raypaths for S phases used in this study. (For interpretation of the references to color in this figure legend, the reader is referred to the web version of this article.)

detailed SK(K)S splitting analysis, we identified 16 stations (14 null and 2 with simple SK(K)S splitting) suitable for probing the Scotia sub-slab mantle, of which 14 actually yielded source-side splitting measurements, and 20 stations (12 null and 8 simple) to study the Caribbean, of which 17 yielded source-side measurements (Fig. 2). Of the 108 candidate stations, 76 were not used for the source-side measurements because the SK(K)S splitting patterns were too complex or the backazimuthal coverage was insufficient to rule out complex receiver-side splitting. After usable stations were identified and the receiver-side anisotropy was well constrained, we applied a correction to all S phases to account for receiver-side anisotropy by rotating and time-shifting the horizontal components (e.g., Russo et al., 2010; He and Long, 2011). A list of all stations considered in this study, along with receiver-side corrections, can be found in Supplementary Table S1.

It is important to understand the potential sources of error when using the source-side method. As discussed above, it is necessary to ensure that the receiver-side anisotropy is correctly assessed and removed, as improper characterization of the receiver-side anisotropy is a major potential source of error. If the complex anisotropic structure beneath the station is misinterpreted as a single, flat lying layer, inaccurate source-side correction may yield incorrect estimates of source-side splitting which actually reflect the complex anisotropic structure on the receiver-side. For this reason, we have put a large amount of effort into constraining the receiver-side anisotropy for the stations used in this study, and have restricted our station selection to stations which have good backazimuthal coverage for SK(K)S phases and exhibit simple SK(K)S splitting patterns. Another potential source of error comes from the use of SK(K)S phases to characterize the anisotropy beneath the receiver and correct the direct S phases for receiver-side effects. S and SKS phases sample the upper mantle beneath the receiver-side similarly but not identically; SK(K)S phases have incidence angles of $\sim 6°$–$16°$ while the teleseismic S waves have incidence angles of $\sim 24°$–$37°$. This difference may introduce errors; however, unusually strong and/or complex anisotropic structure would be necessary for this difference in incidence angle to have a strong effect on the measurements. A third potential source of error is the possible misalignment of horizontal seismometer components, which can cause systematic errors in shear wave splitting measurements (e.g., Tian et al., 2011; Hanna and Long, 2012; Lynner and Long, 2012). We identified a systematic misalignment of the horizontal components for several stations used in this study (BGCA, DBIC, ITHO, LVZ, MAHO, MPG, PVAQ, RER, VSU) based on polarization analysis of the SK(K)S phases and corrected for the observed misalignments before measuring splitting. Corrections for the misalignments can be found in Supplementary Table S1.

### 3.2. Data selection and splitting measurements

We identified and measured direct S phases originating from slab earthquakes of magnitude Mw > 5. We applied a bandpass filter to all direct S waveforms to retain energy between 0.04 and 0.125 Hz (the same filter was applied to SK(K)S phases during the station selection process). This filter was chosen to be suitable for application to both direct S and SK(K)S phases, retaining the signal at characteristic periods of SK(K)S phases (~ 10 s) while eliminating noise at periods shorter than 8 s. We measured splitting using the Splitlab software package (Wüstefeld et al., 2007). We visually inspected each waveform to ensure good signal-to-noise ratios. The noisiest arrivals retained in the source-side dataset had an SNR of the radial component of ~ 2, while the majority of the arrivals had SNRs > 3. As initial polarizations are not constrained by the source-receiver geometry

for direct S waves, we used the rotation correlation and eigenvalue minimization methods to determine the splitting parameters for teleseismic S waves. We applied the rotation correlation and the transverse component minimization methods to measure splitting of the SK(K)S phases.

The simultaneous use of multiple splitting methods to measure the shear wave splitting parameters (fast direction, ϕ, and delay time, δt) has been implemented by several studies and found to produce reliable results (e.g., Wirth and Long, 2010; Long and Silver, 2009b; Huang et al., 2011). We only retained splitting measurements for which the two measurement methods yielded consistent results within the 2σ errors. We assigned each measurement a quality of "good" or "fair"; the S arrivals rated "good" had 2σ rotation correlation errors of less than $\pm 25°$ for ϕ, and ± 0.9 s for δt. "Fair" S measurements had larger errors, up to $\pm 37°$ for ϕ and ± 1.3 s for δt. Null measurement characterizations were based on linearity of the uncorrected particle motion after the receiver-side correction had been made for the teleseismic S waves. A table of all individual source-side measurements made in this study, along with error estimates, can be found in Supplementary Table S2.

4. Results

Shear wave splitting parameters attributed to the sub-slab mantle beneath the Scotia and Caribbean subduction zones are shown in map view in Figs. 3 and 4. Maps of null measurements
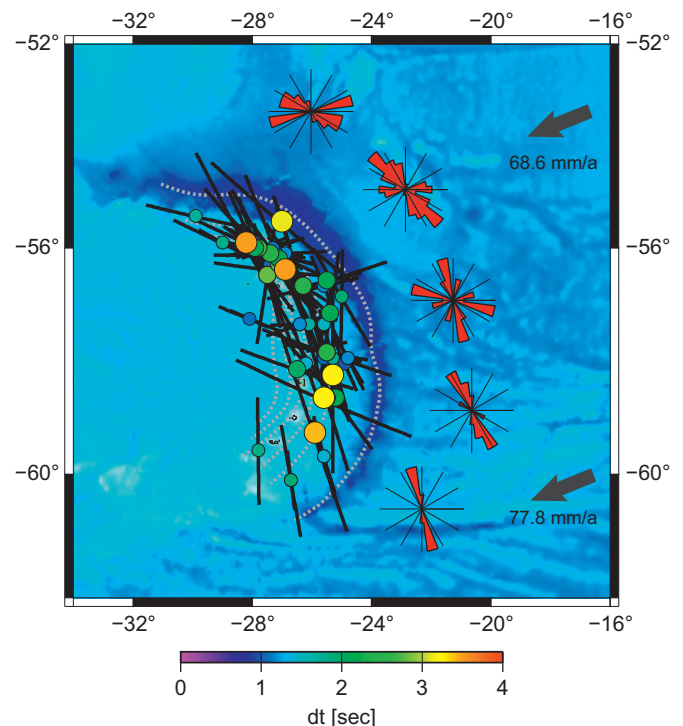
Fig. 3. Results for the Scotia source-side splitting study. Source-side splitting parameters attributed to sub-slab anisotropy are plotted at the earthquake location, with colors indicating the splitting delay times. The orientation of black lines denote the fast splitting direction, while their lengths are scaled by the delay time. Black arrows show relative plate motions. Dashed lines show contours of slab seismicity, in intervals of 50 km, from Gudmundsson and Sambridge (1998). Rose plots are circular histograms of the distribution of fast splitting directions (bin size 15°); each rose plot covers a different segment of the subduction zone (less than 56° latitude, 56°–57° latitude, 57°–58° latitude, 58°–60° latitude, and greater than 60° latitude). A pattern of dominantly trench parallel fast splitting directions can be seen in the northern portion of the trench, while in south, no such pattern is apparent. (For interpretation of the references to color in this figure legend, the reader is referred to the web version of this article.)
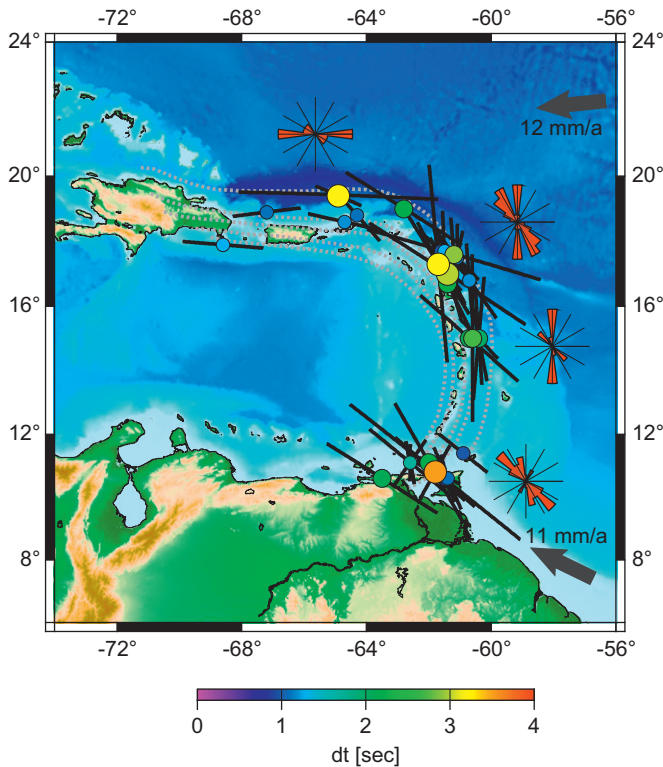
Fig. 4. Results for the Caribbean source-side splitting study. Source-side splitting parameters are plotted using the same conventions as Fig. 3. Rose plots are circular histograms of the distribution of fast splitting directions (bin size 15°); each rose plot covers a different segment of the subduction zone (the northernmost region where curvature is minimal, 16°–18° latitude, 14°–16° latitude, and less than 12° latitude). A clear pattern of trench-parallel splitting is seen in the northern portion of the trench. In the southern region, there is a strong and consistent splitting that is roughly trench perpendicular and aligns well with the motion of the subducting plate.

for both subduction zones are shown in Supplementary Figs. S1 and S2. The abundant seismicity of the Scotia slab yielded many high-quality splitting measurements. With 139 recorded "good" or "fair" measurements (95 non-null measurements and 44 null measurements), the pattern of anisotropy beneath the downgoing slab can be studied in great detail. The Scotia sub-slab mantle shows a complicated pattern of anisotropy with a fair amount of scatter in the data (Fig. 3). To first order, the northern portion of the subduction zone is dominated by trench-parallel or sub-parallel fast splitting directions, which is consistent with the dominant global pattern in other subduction zones (Long and Silver, 2009a). We observe a gradual transition to a more complicated pattern of splitting in the southern part of the subduction zone, with a mix of trench-perpendicular, trench-parallel and trench-oblique fast directions. There are substantially fewer results from the southern region as there is less seismicity in the southern area. Delay times range from ~0.5 s up to ~3.5 s, with an average delay time of 1.6 s (obtained via a simple, non-weighted average). There are no obvious spatial patterns in the observed delay times.

The Caribbean slab exhibits less seismicity than Scotia, but our analysis yielded 60 "good" and "fair" measurements (46 non-null measurements and 14 null measurements). We see similar patterns of sub-slab splitting beneath the Caribbean as we observe in Scotia, but there is significantly less scatter in the measurements and the spatial patterns are better defined (Fig. 4). The northern and central parts of the Caribbean subduction zone show strongly trench-parallel fast splitting directions, with fast directions following the curve of the trench as it bends to the north. There is a gap in our data coverage between ~14°N–11°N

that corresponds to the gap in slab seismicity; to the south of that gap, we observe strong and consistent splitting with dominantly trench-perpendicular fast directions and only a few trench-parallel or trench-oblique ϕ. The group of measurements at the southern edge of the Caribbean subduction zone yields average splitting parameters of $\phi = -27°$ and $\delta t = 1.2$ s. Sub-slab delay times beneath the Caribbean are slightly smaller, on average, than beneath Scotia, with an average delay time of 1.4 s compared to Scotia's 1.6 s.

Given the amount of scatter in the data, particularly for Scotia, we were careful to confirm that when a single event yielded measurements at multiple stations, the splitting parameter estimates were generally consistent with each other. Fig. 5 illustrates several instances in which the same event yields similar splitting parameters at different stations at different epicentral distances and backazimuths from the source region. This confirms the accuracy of the receiver-side station corrections and gives us confidence in our source-side measurement method. We therefore attribute the scatter in the splitting measurements observed beneath Scotia to possible complex anisotropy beneath the source region (e.g. multiple layers of anisotropy, anisotropy with a dipping symmetry axis); in this scenario raypaths sampling the anisotropic structure with different geometries would reflect different apparent splitting. As discussed below, we may be able to use evidence for such complexity in the source region to test different models proposed for sub-slab mantle dynamics.

Complexity in the source region may present itself in several different ways, and it is important to assess whether there are systematic variations in delay times or fast directions with respect to variables such as event depth or raypath parameters such as takeoff angle. We have interrogated our data set to explore such variations, as shown in Figs. 6 and 7. Here we plot measured fast directions (more specifically, the difference between the measured fast direction and the local trench strike) as a function of event depth and ray propagation angle (more specifically, the angle between the ray takeoff angle and a vector normal to the plane of the slab, here defined as the "takeoff angle"). We also plot measured delay times as a function of these two variables. Fig. 6 shows all the splitting data sets while in Fig. 7 we plot only the most well constrained measurements (2σ errors smaller than ± 0.5 s for δt and less than $\pm 20°$ for ϕ). We might expect to see a decrease in delay times with increasing event depth if the S waves are sampling a smaller anisotropic layer beneath the subducting slab with increasing event depth, as has been observed for other source-side splitting datasets (e.g., Foley and Long, 2011). Such a decrease with depth is not apparent in this dataset, likely in part because most of the events are from depths shallower than 100 km and our data set does not have good coverage for deeper events. We do not observe any apparent trend in δt or ϕ and either event depth or takeoff angle when the entire dataset is considered (Fig. 6). When only the most well constrained measurements are used, trends between δt or ϕ with event depth or between ϕ and takeoff angle are still absent, but we do observe a weak trend of decreasing δt with decreasing takeoff angle (Fig. 7). As discussed in Section 5.2 below, any observed relationships (or lack thereof) between splitting observations and raypath parameters may be used to test the predictions of different models for sub-slab anisotropy; the plots shown in Figs. 6 and 7 are discussed in further detail below.

Our results are consistent with results from previous studies that examined sub-slab anisotropy in the Scotia and Caribbean subduction zones (Fig. 8). Müller et al. (2008) examined sub-slab shear wave splitting in the Scotia subduction zone using the source-side splitting technique applied to ScS phases. They used two seismic stations to examine the sub-slab anisotropy and their analysis yielded ~30 measurements. They found evidence for
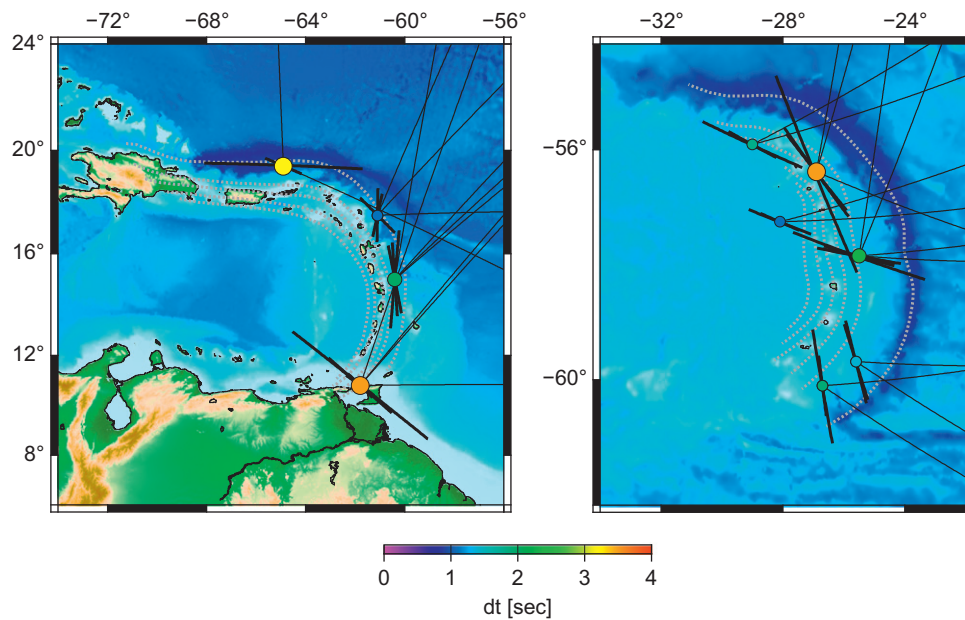
Fig. 5. Map view of several examples in which a single source earthquake yielded splitting parameter estimates at several different stations for the Caribbean (left) and Scotia (right). Splitting parameters are plotted at the event location. Length of the lines scale with delay time and their orientation corresponds with the fast axis. Thin lines leaving the points denote the great circle paths from the sources to the stations at which the measurements were recorded. Each subduction zone has many instances where splitting parameters for a single event agree well between different stations. In a few instances, the agreement between different stations is less good, particularly for the northern-most event in the Caribbean, which exhibits similar fast direction estimates but very different delay time estimates.
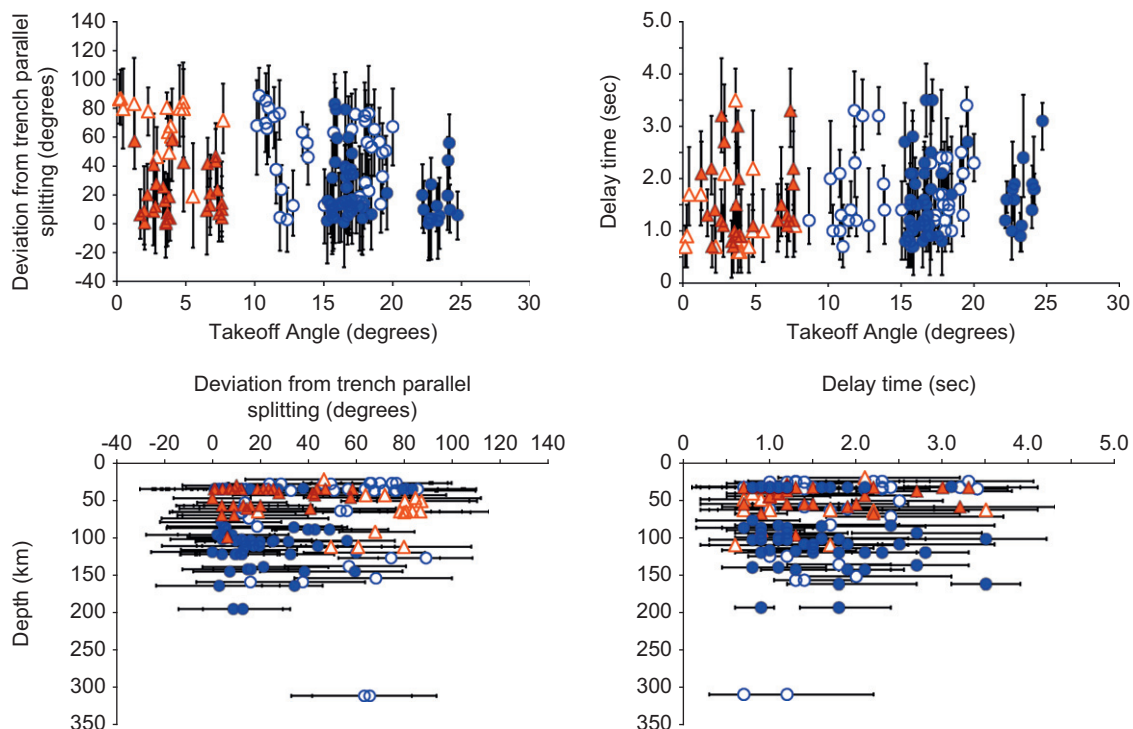

Fig. 6. Plots showing variation of splitting parameters with event depth and angle between the downgoing ray and the subducting slab dip. The takeoff angle (relative to the slab dip) of each downgoing ray in the upper mantle was estimated from the event location and the pierce point at the 410-km discontinuity, calculated using the TauP algorithm (Crotwell et al., 1999) for the iasp91 earth model (Kennett and Engdahl, 1991). Slab dip values were taken from Schellart (2007) using the shallow dip values, dip at depths less than 150 km, and range between 32°–39° for the Caribbean and 50°–56° degrees for Scotia. Red triangles represent individual splitting measurements from the Caribbean subduction zone, while blue circles represent individual splitting measurements from Scotia. Open triangles and circles represent measurements from the southern regions of the Caribbean and Scotia subduction zones. We show all splitting results with their corresponding 2-σ errors for both fast directions and delay times. Top left: Angle between the measured fast splitting direction and the local slab strike, estimated from the 50 km slab depth contour, plotted as a function of the angle between the downgoing ray and the slab dip. Top right: Delay times versus the angle between the downgoing ray and the slab dip. Bottom left: Angle between measured fast splitting direction and the local slab strike plotted as a function of event depth. Bottom right: Delay times versus event depth. (For interpretation of the references to color in this figure legend, the reader is referred to the web version of this article.)
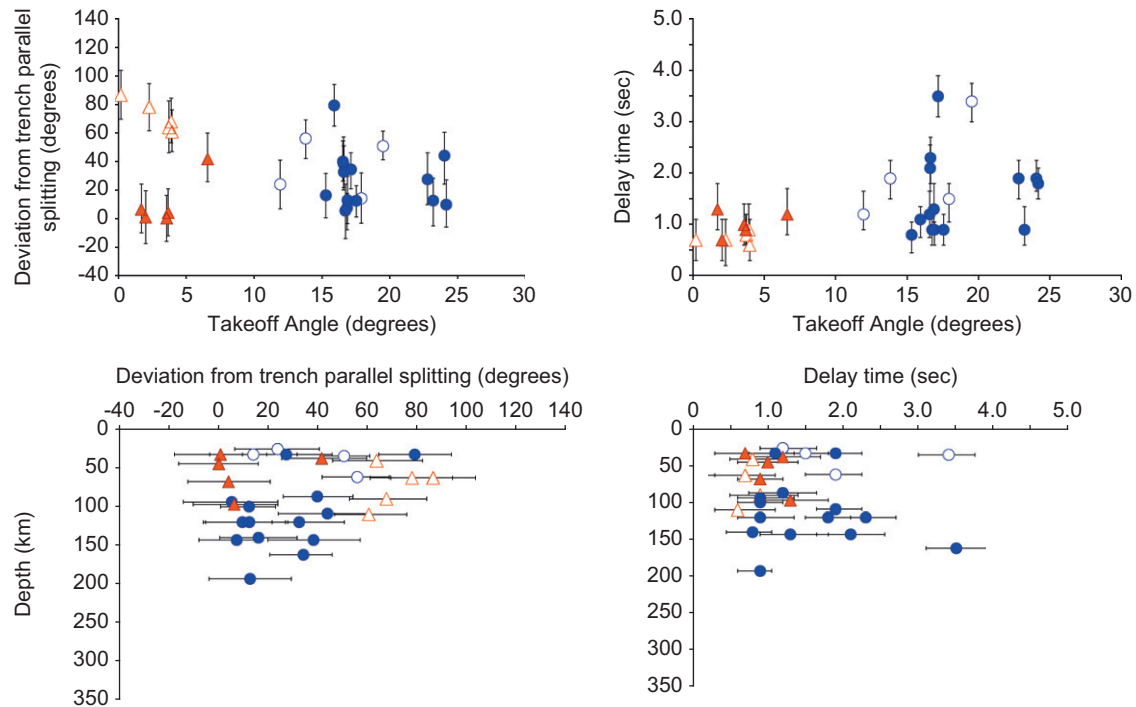
Fig. 7. Plots showing variation in splitting parameters with takeoff angle and depth. Plotting conventions are the same as in Fig. 6. Plotted are only our most robust individual source-side splitting measurements, those with delay time errors smaller than ± 0.5 s and fast axis errors less than $\pm 20°$. As was seen in Fig. 6, there is no discernable systematic variation between depth or takeoff angle and ϕ or depth and δt. A weak trend of increasing δt with increasing takeoff angle is discernible.
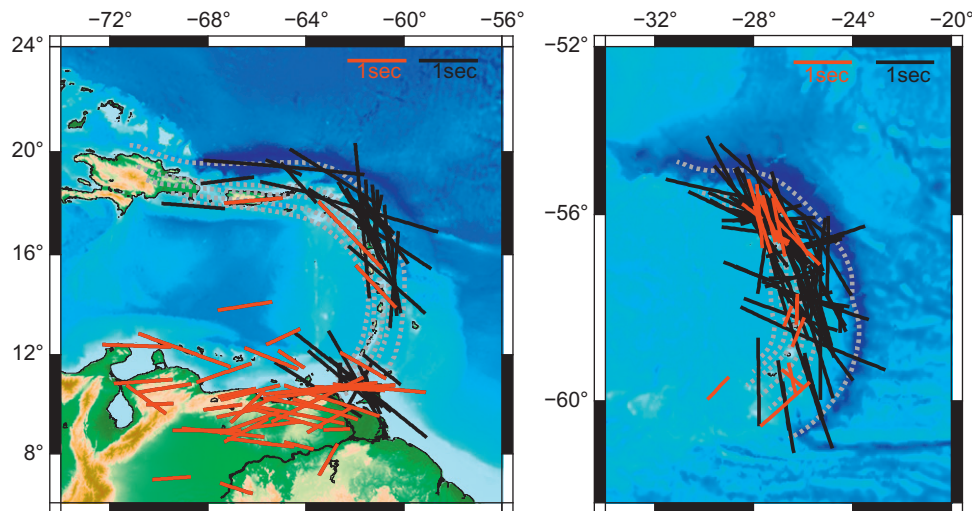
Fig. 8. Results of Caribbean (Right) and Scotia (Left) source-side splitting studies (black bars) plotted with results from previous shear wave splitting studies (red bars). Plotted are the source-side splitting results from Müller et al. (2008) for Scotia as well as results from SK(K)S splitting studies in the Caribbean region from Russo et al. (1996), Piñero-Feliciangeli and Kendall (2008), and Growdon et al. (2009). All individual source-side measurements are plotted such that the mid-point of the bar is plotted at the earthquake location. All SK(K)S measurements are station averages reported in the respective studies and are plotted such that the mid-point of the bar corresponds with the station location. Orientation and lengths of the bars correspond to fast axis and delay time, respectively, with delay time denoted in the upper right corners.

trench-parallel ϕ in the northern and central parts of the subduction zone, with a more complicated pattern of splitting in the south and a few instances of trench perpendicular fast directions from deep events. The Caribbean sub-slab mantle was previously studied by Piñero-Feliciangeli and Kendall (2008) using SK(K)S phases at seismic stations located on three of the Caribbean islands. Because their study used SK(K)S phases, there is a potential contribution from the mantle wedge, although Piñero-Feliciangeli and Kendall (2008) used local S splitting measurements to argue that splitting due to wedge anisotropy is small. This study also showed a generally trench parallel splitting pattern in the northern part of the subduction zone,

consistent with our fast direction results. It is notable that average SK(K)S delay times observed by Piñero-Feliciangeli and Kendall (2008) in the region just north of the seismicity gap are smaller than those seen in our source-side dataset, ~ 1.2 s and ~ 1.6 s respectively. There are two potential explanations for this discrepancy. There may be an effect of destructive interference between anisotropy in the sub-slab mantle and anisotropy elsewhere in the system (such as the slab, the wedge, or the overriding plate) that is sampled by SK(K)S phases. Alternatively, there may be an effect from complex anisotropic structure at depth that is imperfectly sampled by an SK(K)S dataset with limited backazimuthal coverage. Because of the limited station

coverage, Piñero-Feliciangeli and Kendall (2008) were not able to constrain sub-slab mantle anisotropy in the southern part of the subduction zone.

We have also compared our results to other shear wave splitting studies in the Caribbean region. In particular, Russo et al. (1996) and Growdon et al. (2009) have examined SK(K)S splitting in the southern region of the Caribbean subduction zone as well as the region along the plate boundary in Venezuela (Fig. 8). Along the plate boundary in Venezuela, SK(K)S fast directions are roughly parallel to the plate boundary, but the source-side measurements from this study do not extend into this region. In the southern region of the subduction zone, adjacent to our observations of strong trench-perpendicular splitting, Russo et al. (1996) and Growdon et al. (2009) observe generally E–W fast SK(K)S splitting directions that locally align with the Bocono Fault. One station in the Growdon et al. (2009) study located close to our study region exhibits trench-perpendicular ϕ, similar to what we see in the source-side measurements. An important caveat with these types of comparisons, however, is that SK(K)S measurements are not directly comparable to source-side measurements as they are sampling different portions of the subduction zone system, as discussed above in Section 3.1.

5. Discussion

5.1. Comparison of Scotia and Caribbean sub-slab splitting

The sub-slab splitting patterns observed in both the Scotia and Caribbean subduction zones are striking. Both subduction zones appear to be dominated by trench-parallel fast directions along much of their length, but both subduction zones also have a group of splitting measurements at their southern ends that deviate from this trench-parallel pattern. In the Caribbean, the southern-most end is dominated by trench-perpendicular ϕ, while for Scotia the southern portion exhibits a mix of fast directions, with trench-oblique ϕ at the southernmost end. There is a striking correspondence between the morphologies of the Caribbean and Scotia slabs and the observed fast direction patterns, with fast directions in the northern portions of both subduction zones following the curve of the trench, appearing to "wrap" around the slab.

A key question in the interpretation of our results is whether our measurements primarily reflect anisotropy within the sub-ducting slab itself or in the sub-slab mantle. The raypaths used in this study sample both parts of the subduction system, so there is likely some contribution from both. Based on the large delay times we observe and the relatively short (~60–80 km) path lengths through the slab itself for most S phases measured in this study, it is likely that the bulk of the contribution comes from the sub-slab mantle (e.g., Long and Silver, 2009a), where path lengths are much longer (~100–300 km). While some studies have identified observational evidence for significant fossil anisotropy in a subducting slab (e.g., Hammond et al., 2010), such data sets usually use shear wave arrivals with considerably longer path lengths in the slab than we have in our data set. We note, additionally, that the dominantly trench-parallel fast directions we observe are not consistent with the expected signature from fossil anisotropy in the slab lithosphere, given the geometry of spreading that formed the lithosphere that is now subducting beneath Scotia and the Caribbean. Therefore, while a contribution from fossil anisotropy within the slab cannot be ruled out completely, anisotropy in the sub-slab mantle is the most likely primary contributor to the observed splitting. A possible contribution to source-side splitting from aligned serpentinized

cracks in the shallow part of the subducting slab is discussed further in Section 5.2 below.

Most subduction zones worldwide exhibit trench-parallel or sub-parallel fast splitting directions in the sub-slab mantle (Long and Silver, 2008, 2009a). The northern portions of both the Caribbean and Scotia subduction zones agree with this observation, with the Caribbean in particular showing a very clear trench parallel splitting pattern. Several different hypotheses have been proposed to explain the cause of trench-parallel sub-slab fast splitting directions observed in many subduction zones. In the sections below, we discuss these hypotheses and evaluate them in light of the detailed dataset of sub-slab splitting we have produced for the Scotia and Caribbean slabs. We also discuss the deviations from trench-parallel ϕ that we observe in the southern portions of both subduction zones and interpret these observations in terms of the kinematics and tectonic setting of each slab edge.

5.2. Hypothesis testing of different models for sub-slab anisotropy

Several models have been proposed to explain the unexpected observation of dominantly trench-parallel fast splitting directions in subduction zones worldwide. A simple model of 2-D entrained flow, in which the sub-slab mantle is dragged along with the downgoing plate, would predict trench-perpendicular ϕ for the case of hexagonal anisotropy with a dipping fast symmetry axis (Russo and Silver, 1994), consistent with most olivine LPO scenarios (e.g., Karato et al., 2008). Models which would correctly predict the observed trench-parallel ϕ include those that invoke trench-parallel sub-slab mantle flow (Russo and Silver, 1994; Long and Silver, 2008, 2009a), a pressure-induced transition to olivine B-type fabric (Jung et al., 2009), the effect of serpentinized cracks in the subducting slab (Faccenda et al., 2008, Healy et al., 2009), and the entrainment of a layer of suboceanic astheno-sphere with strong radial anisotropy (Song and Kawakatsu, 2012).

The B-type olivine fabric model proposed by Jung et al. (2009) invokes experimental evidence for a pressure transition in olivine fabric such that B-type olivine is dominant at pressures greater than ~3 GPa (corresponding to depths of ~80–90 km). The geometry of olivine B-type fabric is such that the fast axis of olivine tends to align perpendicular to the direction of maximal extensional strain, a 90° difference from A-type olivine fabric. Jung et al. (2009) suggested that B-type olivine fabric beneath slabs might provide an explanation for trench-parallel fast split-ting observations without needing to invoke a deviation in mantle flow from the 2-D entrained flow scenario. However, the B-type fabric model is difficult to reconcile with some seismological and petrographic observations, such as the good match between fast directions and plate motions in ocean basins (e.g. Conrad et al., 2007), and olivine fabrics from xenoliths formed at pressures greater than 3 GPa (e.g. Ben Ismaïl and Mainprice, 1998). One testable prediction of the Jung et al. (2009) model is that there should be a striking transition in splitting behavior at an event depth of ~80–90 km, as S phases originating above and beneath this depth should sample different combinations of olivine fabrics. The plot of splitting behavior as a function of event depth shown in Figs. 6 and 7 demonstrates that we do not observe such a transition in our data set, and such a transition has not been observed in other source-side splitting studies (Müller et al., 2008; Foley and Long, 2011). We therefore rule out the B-type pressure transition model as a likely explanation for the Scotia and Caribbean observations.

The serpentinized crack model, advocated by Faccenda et al. (2008) and Healy et al. (2009), suggests that trench-parallel SKS fast directions are caused by aligned cracks in the subducting slab containing highly anisotropic serpentinite minerals, leading

to a combined lattice preferred orientation (LPO) and shape preferred orientation (SPO) effect. In the context of this model, one would expect dominantly trench-parallel splitting for S phases that sample the shallow part of the Scotia and Caribbean slabs, with a transition to null splitting for events that originate below the serpentinite stability field (~100 km; Ulmer and Trommsdorff, 1995). Such a sharp transition in splitting behavior is not observed in our data set (Figs. 3, 4, 6, and 7) or in other regions such as Tonga (Foley and Long, 2011). Therefore, while we cannot completely rule out a contribution to the observed splitting from this mechanism, it appears that we can rule it out as the primary mechanism for anisotropy in the Scotia and Caribbean regions.

This leaves the 3-D return flow model (Long and Silver, 2008, 2009a) and the entrained asthenosphere model (Song and Kawakatsu, 2012) as viable mechanisms to explain our observations. To first order, each of these models predicts dominantly trench-parallel sub-slab fast splitting directions, but as discussed below, the detailed predictions about splitting behavior as a function of variables such as raypath takeoff angle are different for the two models. The key advantage of the detailed sub-slab splitting datasets we have generated for Scotia and the Caribbean is that they can be used to rigorously test the predictions of these two different models.

The Song and Kawakatsu (2012) model proposes that the oceanic asthenosphere is everywhere characterized by strong radial anisotropy as well as a weak component of azimuthal anisotropy. As the oceanic lithosphere is subducted, it entrains a layer of anisotropic asthenosphere beneath it. Once a critical slab dip angle is reached, the strong radial component of anisotropy gives rise to trench parallel fast splitting directions for (nearly) vertically propagating waves. One way to test the predictions of this model in the context of our source-side splitting data set is to examine our measurements for any specific trends predicted by the model for different raypath configurations. The Song and Kawakatsu (2012) model predicts a systematic variation in splitting parameters with the takeoff angle of the S raypaths (or, more precisely, with the angle between the downgoing seismic ray and the dip of the subducted slab). Specifically, the model predicts a transition from trench-parallel to trench-perpendicular fast directions for shallower slab dip angles (or, equivalently, for shallower takeoff angles) and also predicts a systematic decrease in delay times with depth for slab dips or takeoff angles that remain in the trench-parallel regime. This prediction can be tested for our Scotia/Caribbean data set using the plots shown in Figs. 6 and 7. We do not observe any systematic variation in splitting parameters with takeoff angle or event depth when the entire dataset is taken into account (Fig. 6). Systematic variations in δt or ϕ with depth or systematic variation in ϕ with takeoff angle are still absent when only the best-constrained measurements are used (Fig. 7).

It is important to note that the variations predicted by the model of Song and Kawakatsu (2012) could be masked by the amount of scatter in our measurements, particularly for Scotia. Given the lack of systematic variation in ϕ with takeoff angle, it appears that an entrained asthenospheric sub-slab layer with strong radial anisotropy cannot explain all the features of our splitting dataset, although it cannot be completely ruled out. An important avenue for future work is a detailed comparison between the predictions of the Song and Kawakatsu (2012) model and individual measurements in our data set.

Our preferred model to explain the strong trend of trench-parallel fast directions seen in the northern portions of both subduction zones is that it is due to lateral flow of the sub-slab mantle around the edges of the subducting slabs induced by trench migration as advocated by Russo and Silver (1994) for

South America and by Long and Silver (2008, 2009a) as a global phenomenon. Both the Caribbean and Scotia subduction zones are undergoing slab rollback relative to the South American plate and are prime locations to examine the potential influence of rollback on the sub-slab mantle. In the context of the slab rollback model, the migration of the Scotia and Caribbean trenches and the motion of the slabs may induce a toroidal flow field around the edges of the highly curved subducting slabs. This mechanism has previously been suggested to explain anisotropy measurements beneath Scotia (Müller et al., 2008) and has also been invoked to explain patterns of trench-parallel sub-slab splitting in other highly curved subduction zones such as Calabria (Civello and Margheriti, 2004). Recent numerical modeling work (Paczkowski, 2012) has demonstrated that when slabs are decoupled from the mantle beneath them and rollback induces trench-parallel sub-slab mantle flow, the resulting finite strain pattern is dominated by trench-parallel maximum extension directions with horizontal axes of symmetry. If this finite strain pattern is a reasonable proxy for the geometry of anisotropy (e.g., Ribe, 1992; Lev and Hager, 2008), then we would expect a single layer of sub-slab anisotropy with a horizontal symmetry axis aligned with the trench. This type of model can generally explain the observations in the northern portions of the Scotia and Caribbean subduction zones, and for this scenario we would not expect to see large variations in ϕ with ray angle (Figs. 6 and 7).

Both the Song and Kawakatsu (2012) model and the 3D return flow model predict a general trend of increasing δt with increasing takeoff angle; such a trend can be seen in Fig. 7, although it is weak. In the Song and Kawakatsu (2012) model, this predicted trend is due to the increasing strength of radial (as opposed to azimuthal) anisotropy experienced by a wave as takeoff angle increases. (We note, however, that an accompanying change in ϕ as takeoff angle increases is not seen.) In the 3D return flow model, as takeoff angles increase, raypaths in the sub-slab mantle lengthen and propagating S waves should build up larger delay times.

5.3. Our preferred model for sub-slab mantle flow beneath Scotia and the Caribbean

The trench-parallel sub-slab flow model can explain the bulk of our observations in the northern portions of both subduction zones, but it does not provide a ready explanation for the deviations from trench-parallel ϕ at the southern ends of both regions. Here we consider the kinematic and tectonic settings of each subduction system and propose conceptual models for mantle flow beneath both slabs that are consistent with the observations. In both subduction systems, the mostly likely scenario is that sub-slab mantle flow is being driven preferentially from the south to the north around the slab by trench rollback. Given the differences in tectonic setting between the two systems, however, the south-to-north flow is likely being driven by different phenomena.

In the Caribbean subduction zone (Fig. 9), we propose that the tectonic setting at the southern end of the slab restricts mantle flow around its southern edge. Immediately to the south of the Caribbean slab edge lies the South American continent, which has a thick continental lithospheric root (Masy et al., 2011; Niu et al., 2007; Growdon et al., 2009; Miller et al., 2009; Russo et al., 1996). We hypothesize that this thick continental root partially or fully blocks the escape route for mantle flow around the southern end of the slab, forcing mantle to flow preferentially to the north as the slab rolls back. Station coverage in the region immediately adjacent to the boundary between the Caribbean and South American plates has been poor until recently (e.g., Heintz et al., 2005), but recent surface wave models indicate that the upper mantle structure in northern Venezuela is complex
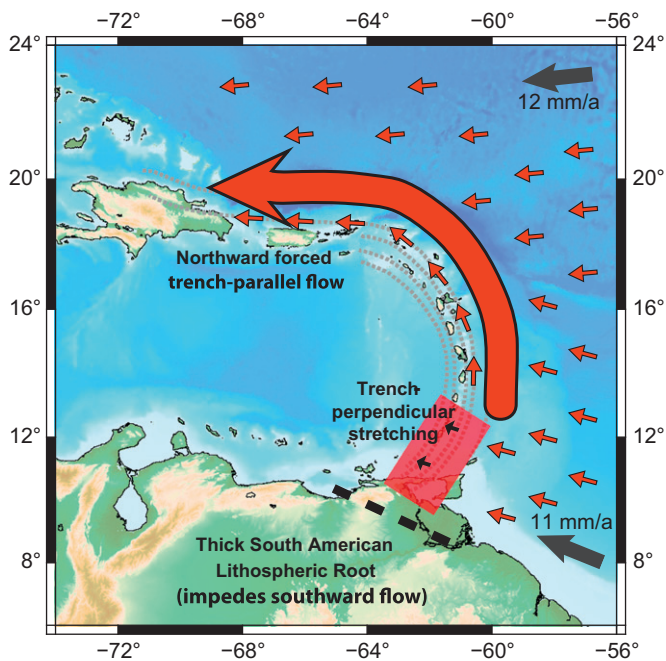
Fig. 9. Cartoon sketch of our preferred model for sub-slab mantle flow in the Caribbean subduction zone. Black arrows represent plate convergence directions; short red arrows represent the likely geometry of upper mantle shear beneath the downgoing plate. The thick red arrow represents likely geometry of sub-slab mantle flow. The thick lithospheric root of the South American continent acts as a barrier to flow (thick black dotted line) around the southern edge of the slab. Therefore, the rollback motion of the slab causes the sub-slab mantle to flow preferentially to the north. In the southern region (red rectangle), local trench-perpendicular stretching due to trench migration or local entrained sub-slab flow due to efficient slab-mantle coupling produces trench-perpendicular fast splitting directions. (For interpretation of the references to color in this figure legend, the reader is referred to the web version of this article.)

the slab (Fig. 9). Reconciling these different views of sub-slab flow at the southern edge of the Caribbean subduction system, and in particular investigating whether trench-perpendicular sub-slab ϕ can be reconciled with the flow scenario responsible for splitting observations in northern Venezuela, represents an important area for future investigation.

In contrast to the Caribbean, the Scotia slab lies in a completely intraoceanic setting and there are no obvious barriers to mantle flow at its southern edge. We hypothesize instead that the particular kinematics of the Scotia trench tends to preferentially drive mantle flow to the north. Compilations of trench migration data (Heuret and Lallemand, 2005; Funiciello et al., 2008; Schellart et al., 2008) indicate that the Scotia trench is experiencing differential trench rollback rates from the north to the south and that this pattern is generally independent of which reference frame is used. The middle portion of the trench is rolling back substantially faster than the northern portion (Fig. 10), with the rollback rate systematically decreasing to the north from a latitude of about $58°$ S northwards. We hypothesize that this pattern of differential rollback may be preferentially forcing sub-slab mantle flow northward around the subducting slab.

In the Scotia subduction zone, unlike in the Caribbean, flow southward is not completely inhibited in this scenario; the differential trench rollback merely facilitates flow northward. Instead, we hypothesize that flow around the southern edge of the slab is weaker and less coherent than elsewhere in the subduction system. In such a flow regime, olivine LPO may be less well oriented and the resulting anisotropy may be more complex, resulting in complicated shear wave splitting behavior. This, in turn, may explain the more complicated splitting patterns we observe in southern Scotia, with a mix of trench-parallel, -perpendicular, and -oblique ϕ.

In our preferred model, the patterns of flow in the sub-slab mantle beneath the Caribbean and Scotia subduction zones are

(Miller et al., 2009). Just to the south, the lithosphere beneath the Guyana Shield is thick, extending to depths of $\sim$200–250 km (Lebedev et al., 2009). The detailed structure of the lithosphere directly to the south of the Caribbean slab edge is imperfectly known, but it is plausible that the continental lithosphere may block, deflect, or otherwise modify sub-slab flow around the southern slab edge. The trench-perpendicular fast directions we observe at the southern edge of the Caribbean slab may be due to a modest amount of local trench-perpendicular stretching in the mantle as the mantle material is forced to the east by the migration of the slab. Alternatively, the trench-perpendicular ϕ, which are also roughly parallel to the motion of the downgoing plate, may reflect local entrained flow beneath the slab if the slab is locally coupled to the subjacent mantle.
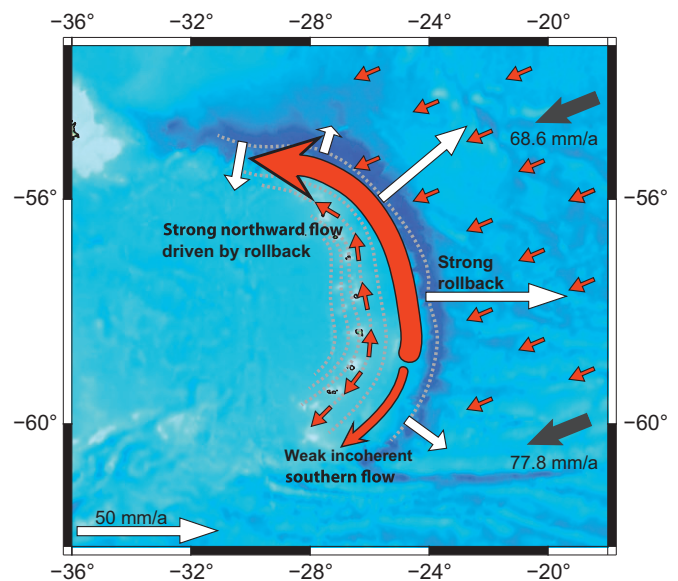
Our inference that flow around the southern edge of the slab may be impeded by the presence of the South American continental lithosphere contrasts somewhat with a class of models that have been proposed to explain the pattern of shear wave splitting and upper mantle velocities in northern Venezuela, which invoke three-dimensional flow around the southern slab edge (e.g., Growdon et al., 2009; Miller et al., 2009; Miller and Becker, 2012). In particular, the numerical modeling study of Miller and Becker (2012) proposes that the interaction of mantle flow around the southern edge of the Caribbean slab with the South American continental keel results in channelized flow beneath the transform plate boundary in northern Venezuela. While our preferred flow scenario shares a conceptual similarity in that we also invoke the effect of the continental keel on mantle flow, in our model flow around the southern edge is significantly impeded, resulting in trench-perpendicular stretching beneath

Fig. 10. Cartoon sketch of our preferred model for sub-slab mantle flow in the Scotia subduction zone. Black arrows represent plate convergence directions; short red arrows represent the likely geometry of upper mantle shear beneath the downgoing plate. The thick red arrow represents likely geometry of sub-slab mantle flow. The white arrows denote rollback rates for different portions of the subduction zone from Funiciello et al. (2008) in the hot spot reference frame of Gordon and Jurdy (1986), with reference velocity in lower left-hand corner. The differential rollback of the subducting slab preferentially forces the sub-slab mantle northward without completely preventing southward flow. (For interpretation of the references to color in this figure legend, the reader is referred to the web version of this article.)

similar, yet different processes are controlling the flow. We hypothesize that in the Caribbean, the presence of the thick South American continental lithosphere inhibits flow around the southern edge, while in Scotia, flow is being driven preferentially to the north as a consequence of the differential trench migration rates. This difference in inferred mechanism highlights the importance of plate kinematics and tectonic setting in controlling sub-slab mantle flow in individual subduction zones. A key question related to the dynamics of these subduction systems that remains unanswered by this study is to what extent a highly curved slab morphology influences mantle flow around slab edges or, conversely, whether toroidal flow around slab edges causes high slab curvature. Does a highly curved slab make toroidal flow around slab edges more dynamically favorable and thus result in well-organized patterns of sub-slab fast splitting directions that parallel the trench curvature? Or does efficient toroidal flow due to slab rollback affect slab shapes and result in highly curved slab and trench morphologies? This represents an important question in subduction geodynamics that deserves future study, both from an observational and a geodynamical modeling point of view.

6. Summary

Detailed, high-quality source-side splitting data sets can yield powerful insights into the processes that control flow in the sub-slab mantle. We have presented a set of source-side splitting measurements that probe anisotropy beneath the Scotia and Caribbean slabs. Great care was taken when selecting stations to use in this work, minimizing potential error due to inaccurate corrections for anisotropy beneath the receivers. Our analysis reveals that trench-parallel sub-slab fast splitting directions dominate throughout the northern portions of both subduction systems, but both regions show a deviation from trench-parallel ϕ at their southern ends. We have tested the predictions made by four different models that have been proposed to explain trench-parallel splitting beneath subducting slabs. Our preferred model is that anisotropy beneath the Scotia and Caribbean slabs is mainly controlled by trench-parallel mantle flow induced by trench migration; in both systems, sub-slab mantle is preferentially driven to the north. In the Caribbean, we hypothesize that the presence of the South American continental keel inhibits flow around the southern slab edge, while for Scotia, flow is likely driven preferentially to the north by differential migration of the trench. Our preferred model highlights the importance of local slab kinematics and tectonic setting in controlling sub-slab mantle flow.

Acknowledgments

Appendix A. Supporting information

Supplementary data associated with this article can be found in the online version at http://dx.doi.org/10.1016/j.epsl.2012.11.007.

References

Ben Ismaïl, W., Mainprice, D., 1998. An olivine fabric database: an overview of upper mantle fabrics and seismic anisotropy. Tectonophysics 296, 145–157.

Billen, M.I., 2008. Modeling the dynamics of subducting slabs. Annu. Rev. Earth Planet. Sci. 36, 325–356.

Civello, S., Margheriti, L., 2004. Toroidal mantle flow around the Calabrian slab (Italy) from SKS splitting. Geophys. Res. Lett. 31, L10601, http://dx.doi.org/10.1029/2004GL019607.

Conrad, C.P., Behn, M.D., Silver, P.G., 2007. Global mantle flow and the development of seismic anisotropy: differences between the oceanic and continental upper mantle. J. Geophys. Res. 112, B07317, http://dx.doi.org/10.1029/2006JB004608.

Crotwell, H.P., Owens, T.J., Ritsema, J., 1999. The TauP Toolkit: flexible seismic travel-time and ray-path utilities. Seismol. Res. Lett. 70, 154–160.

DeMets, C., Gordon, R.G., Argus, D.F., Stein, S., 1990. Current plate motions. Geophys. J. Int. 101, 425–478.

Di Leo, J., Wookey, J., Hammond, J.O.S., Kendall, J.-M., Kaneshima, S., Inoue, H., Yamashina, T., Harjadi, P., 2012. Deformation and mantle flow beneath the Sangihe subduction zone from seismic anisotropy. Phys. Earth Planet. Inter. 194–195, 38–54.

Faccenda, M., Burlini, L., Gerya, T.V., Mainprice, D., 2008. Fault-induced seismic anisotropy by hydration in subducting oceanic plates. Nature 455, 1097–1100.

Foley, B.J., Long, M.D., 2011. Upper and mid-mantle anisotropy beneath the Tonga slab. Geophys. Res. Lett. 38, L02303, http://dx.doi.org/10.1029/2010GL046021.

Funiciello, F., Faccenna, C., Heuret, A., Lallemand, S., Di Giuseppe, E., Becker, T.W., 2008. Trench migration, net rotation and slab–mantle coupling. Earth Planet. Sci. Lett. 271, 233–240.

Gordon, R.G., Jurdy, D.M., 1986. Cenozoic global plate motions. J. Geophys. Res. 91, 12389–12406.

Growdon, M.A., Pavlis, G.L., Niu, F., Vernon, F.L., Rendon, H., 2009. Constraints on mantle flow at the Caribbean—South American plate boundary inferred from shear wave splitting. J. Geophys. Res. 114, B02303, http://dx.doi.org/10.1029/2008JB005887.

Gudmundsson, O., Sambridge, M., 1998. A regionalized upper mantle (RUM) seismic model. J. Geophys. Res. 103, 7121–7136.

Hammond, J.O.S., Wookey, J., Kaneshima, S., Inoue, H., Yamashina, T., Harjadi, P., 2010. Systematic variation in anisotropy beneath the mantle wedge in the Java–Sumatra subduction system from shear-wave splitting. Phys. Earth Planet. Inter. 178, 189–201.

Hanna, J., Long, M.D., 2012. SKS splitting beneath Alaska: regional variability and implications for subduction processes at a slab edge. Tectonophysics 530–531, 272–285.

He, X., Long, M.D., 2011. Lowermost mantle anisotropy beneath the northwestern Pacific: evidence from ScS, PcS, SKS, and SKKS phases. Geochem. Geophys. Geosyst. 12, Q12012, http://dx.doi.org/10.1029/2011GC003779.

Healy, D., Reddy, S.M., Timms, N.E., Gray, E.M., Vitale Brovarone, A., 2009. Trench-parallel fast axes of seismic anisotropy due to fluid-filled cracks in subducting slabs. Earth Planet. Sci. Lett. 283, 75–86.

Heintz, M., Debayle, E., Vauchez, A., 2005. Upper mantle structure of the South American continent and neighboring oceans from surface wave tomography. Tectonophysics 406, 115–139.

Heuret, A., Lallemand, S., 2005. Plate motions, slab dynamics and back-arc deformation. Phys Earth Planet Int 149, 31–51.

Huang, Z., Wang, L., Zhao, D., Mi, N., Xu, M., 2011. Seismic anisotropy and mantle dynamics beneath China. Earth Planet. Sci. Lett. 306, 105–117.

Jung, H., Mo, W., Green, H.W., 2009. Upper mantle seismic anisotropy resulting from pressure-induced slip transition in olivine. Nat. Geosci. 2, 73–77.

Karato, S., Jung, H., Katayama, I., Skemer, P., 2008. Geodynamic significance of seismic anisotropy of the upper mantle: new insights from laboratory studies. Annu. Rev. Earth Planet Sci. 36, 59–95.

Kennett, B.L.N., Engdahl, E.R., 1991. Traveltimes for global earthquake location and phase identification. Geophys. J. Int. 105, 429–465.

King, S.D., 2007. Mantle downwellings and the fate of subducting slabs: constraints from seismology, geoid topography, geochemistry, and petrology. Treatise Geophys. 7, 325–370.

Lebedev, S., Boonen, J., Trampert, J., 2009. Seismic structure of Precambrian lithosphere: new constraints from broadband surface-wave dispersion. Lithos 109, 96–111.

Lev, E., Hager, B.H., 2008. Prediction of anisotropy from flow models: a comparison of three methods. Geochem. Geophys. Geosyst. 9, Q07014, http://dx.doi.org/10.1029/2008GC002032.

Long, M.D., Becker, T.W., 2010. Mantle dynamics and seismic anisotropy. Earth Planet. Sci. Lett. 297, 341–354.

Long, M.D., Silver, P.G., 2008. The subduction zone flow field from seismic anisotropy: a global view. Science 319, 315–318.

Long, M.D., Silver, P.G., 2009a. Mantle flow in subduction systems: the sub-slab flow field and implications for mantle dynamics. J. Geophys. Res. 114, B10312, http://dx.doi.org/10.1029/2008JB006200.

Long, M.D., Silver, P.G., 2009b. Shear wave splitting and mantle anisotropy: measurements, interpretations, and new directions. Surv. Geophys. 30, 407–461.

Lynner, C., Long, M.D., 2012. Evaluating contributions to SK(K)S splitting from lower mantle anisotropy: a case study from station DBIC. Côte D'Ivoire. Bull. Seism. Soc. Am. 102, 1030–1040.

Mann, P., Calais, E., Ruegg, J.C., DeMets, C., Jansma, P.E., Mattioli, G.S., 2002. Oblique collision in the northeastern Caribbean from GPS measurements and geological observations. Tectonics 21, 1057, http://dx.doi.org/10.1029/2001TC001304.

Masy, J., Niu, F., Levander, A., Schmitz, M., 2011. Mantle flow beneath north-western Venezuela: seismic evidence for a deep origin of the Mérida Andes. Earth Planet. Sci. Lett. 305, 396–404.

Meade, C., Silver, P.G., Kaneshima, S., 1995. Laboratory and seismological observations of lower mantle isotropy. Geophys. Res. Lett. 22, 1293–1296.

Miller, M.S., Becker, T.W., 2012. Mantle flow deflected by interactions between subducted slabs and cratonic keels. Nat. Geosci. 5, 726–730.

Miller, M.S., Levander, A., Niu, F., Li, A., 2009. Upper mantle structure beneath the Caribbean–South American plate boundary from surface wave tomography. J. Geophys. Res. 114, B01312, http://dx.doi.org/10.1029/2007JB005507.

Müller, C., Bayer, B., Eckstaller, A., Miller, H., 2008. Mantle flow in the South Sandwich subduction environment from source-side shear wave splitting. Geophys. Res. Lett. 35, L03301, http://dx.doi.org/10.1029/2007GL032411.

Niu, F., Bravo, T., Pavlis, G., Vernon, F., Rendon, H., Bezada, M., Levander, A., 2007. Receiver function study of the crustal structure of the southeastern Caribbean plate boundary and Venezuela. J. Geophys. Res. 112, B11308, http://dx.doi.org/10.1029/2006JB004802.

Nowacki, A., Kendall, J.-M., Wookey, J., 2012. Mantle anisotropy beneath the Earth's mid-ocean ridges. Earth Planet. Sci. Lett. 317–318, 56–67.

Paczkowski, K., 2012. Dynamic Analysis of Modifications to Simple Plate Tectonic Theory. Ph.D. Thesis. Yale University, 185 pp.

Peyton, V., Levin, V., Park, J., Brandon, M., Lees, J., Gordeev, E., Ozerov, A., 2001. Mantle flow at a slab edge: seismic anisotropy in the Kamchatka region. Geophys. Res. Lett. 28, 379–382, http://dx.doi.org/10.1029/2000GL012200.

Piñero-Feliciangeli, L., Kendall, J.-M., 2008. Sub-slab mantle flow parallel to the Caribbean plate boundaries: inferences from SKS splitting. Tectonophysics 462, 22–34.

Ribe, N.M., 1992. On the relationship between seismic anisotropy and finite strain. J. Geophys. Res. 97, 8737–8748.

Russo, R.M., Silver, P.G., 1994. Trench-parallel flow beneath the Nazca plate from seismic anisotropy. Science 263, 1105–1111.

Russo, R.M., Silver, P.G., Franke, M., Ambeh, W.B., James, D.E., 1996. Shear-wave splitting in northeast Venezuela, Trinidad, and the eastern Caribbean. Phys. Earth Planet. Int. 95, 251–275.

Russo, R.M., Gallego, A., Comte, D., Moncau, V.I., Murdie, R.E., VanDecar, J.C., 2010. Source-side shear wave splitting and upper mantle flow in the Chile Ridge subduction zone. Geology 38, 707–710.

Russo, R.M., 2009. Subducted oceanic asthenosphere and upper mantle flow beneath the Juan de Fuca slab. Lithosphere 1, 195–205.

Savage, M.K., 1999. Seismic anisotropy and mantle deformation: what have we learned from shear wave splitting? Rev. Geophys 37, 65–106.

Schellart, W.P., 2007. The potential influence of subduction zone polarity on overriding plate deformation, trench migration and slab dip angle. Tectonophysics 445, 363–372.

Silver, P.G., Chan, W.W., 1991. Shear wave splitting and subcontinental mantle deformation. J. Geophys. Res. 96, 16429–16454.

Silver, P.G., Savage, M.K., 1994. The interpretation of shear-wave splitting parameters in the presence of two anisotropic layers. Geophys. J. Int. 119, 949–963.

Silver, P.G., 1996. Seismic anisotropy beneath the continents: probing the depths of geology. Annu. Rev. Earth Planet. Sci. 24, 385–432.

Song, T.-R.A., Kawakatsu, H., 2012. Subduction of oceanic asthenosphere: evidence from sub-slab seismic anisotropy. Geophys. Res. Lett. 39, L17301, http://dx.doi.org/10.1029/2012GL052639.

Tian, X., Zhang, J., Si, S., Wang, J., Chen, Y., Zhang, Z., 2011. SKS splitting measurements with horizontal component misalignment. Geophys. J. Int. 185, 329–340.

Thomas, C., Livermore, R., Pollitz, F., 2003. Motion of the Scotia Sea plates. Geophys. J. Int. 155, 789–804.

Ulmer, P., Trommsdorff, V., 1995. Serpentine stability to mantle depths and subduction-related magmatism. Science 268, 858–861.

van Keken, P.E., 2003. Structure and dynamics of the mantle wedge. Earth Planet. Sci. Lett. 215, 323–338.

Vinnik, L.P., Farra, V., Romanowicz, B., 1989. Azimuthal anisotropy in the Earth from observations of SKS at Geoscope and NARS broadband stations. Bull. Seism. Soc. Am. 79, 1542–1558.

Wessel, P., Smith, W.H.F., 1991. Free software helps map and display data. Eos Trans. Am. Geophys. Un. 72, 441.

Wirth, E., Long, M.D., 2010. Frequency-dependent shear wave splitting beneath the Japan and Izu-Bonin subduction zones. Phys. Earth Planet. Int. 181, 141–154.

Wüstefeld, A., Bokelmann, G., Barruol, G., Zaroli, C., 2007. Splitlab: a shear-wave splitting environment in Matlab. Comp. Geosci. 34, 515–528.

Zhao, D., 2001. Seismological structure of subduction zones and its implications for arc magmatism and dynamics. Phys. Earth Planet. Inter. 127, 197–214.